Article **Journal of Innovative Engineering**
June 2023 Vol.7 No.20 16-21

$Sn_3Sb_2S_6$ thin films for photovoltaic applications

Películas delgadas de $Sn_3Sb_2S_6$ para aplicaciones fotovoltaicas

GONZALEZ-GARZA, Jorge Oswaldo†*, GARCÍA-GUILLEN, Grisel, RÍOS-RAMÍREZ, Bernardino and DE RAMÓN-CONDÉ, Andres

Universidad Politécnica de García, García, Nuevo León, México

ID 1st Author: *Jorge Oswaldo, González Garza* / **ORC ID:** 0000-0002-9821-6947, **CVU CONAHCYT ID:** 248626

ID 1st Co-author: *Grisel, García-Guillen* / **ORC ID:** 0000-0002-5919-7755, **CVU CONAHCYT ID:** 297209

ID 2nd Co-author: *Bernardino, Ríos-Ramírez* / **ORC ID:** 0009-0007-6254-1223, **CVU CONAHCYT ID:** 329047

ID 3rd Co-author: *Andres, De Ramón-Condé* / **ORC ID:** 0009-0007-6653-7563, **CVU CONAHCYT ID:** 1289366

DOI: 10.35429/JOIE.2022.20.7.16.21 Received March 13, 2023; Accepted June 30, 2023

Abstract

Tin antimony sulfide semiconductor thin films have been extensively investigated due to their potential application as absorber in thin films solar cells, to convert solar radiation into electricity (A. Gassoumi, 2011; A. Larbi, 2014; Auttasit Tubtimtae, 2021; D. Abdelkader, 2014; N. Ali, 2015; Nisar Ali S. H., 2013a; Nisar Ali S. H., 2013b; Sebin Devasia, 2020); this is due to the excellent optoelectronic properties and due to abundance of the constituent elements on the earth crust and low toxicity. In this research we studied the effect of heat treatment temperature on the formation and optoelectronic properties of $Sn_3Sb_2S_6$ thin films prepared by the heating of multilayers glass/ SnS/Sb_2S_3 chemically deposited, the results show the formation of the ternary phase at temperatures above 250 °C, increasing the crystallinity of the phase at 325 °C. $Sn_3Sb_2S_6$ thin films show an indirect optical transition with band gaps around 1 eV, and absorption coefficient ~ 10^5 cm^{-1} in the visible range. $Sn_3Sb_2S_6$ thin films show conductivities in the range of 10^{-7} – 10^{-6} Wcm^{-1}, showing an increase in conductivity as the temperature increased. The good optoelectronic properties of this material make it suitable for photovoltaic applications.

Optoelectronic, Semiconductor, Properties

Resumen

Las películas delgadas de materiales semiconductores de la familia de sulfuro de antimonio estaño han sido objeto de investigación debido a su potencial aplicación como absorbedor en celdas solares de película delgada, para la generación de electricidad a partir de la radiación solar (A. Gassoumi, 2011; A. Larbi, 2014; Auttasit Tubtimtae, 2021; D. Abdelkader, 2014; N. Ali, 2015; Nisar Ali S. H., 2013a; Nisar Ali S. H., 2013b; Sebin Devasia, 2020); esto debido a sus excelentes propiedades optoelectrónicas y a que sus elementos constituyentes son abundantes en la corteza terrestre y son de baja toxicidad. En esta investigación se estudió el efecto de la temperatura de tratamiento térmico en la formación y propiedades optoelectrónicas de películas delgadas de $Sn_3Sb_2S_6$ preparadas mediante el calentamiento de multicapas de vidrio/SnS/Sb_2S_3 preparadas mediante la técnica de baño químico, los resultados muestran la formación de la fase ternaria a temperaturas superiores a 250 °C, aumentando su cristalinidad a una temperatura de 325 °C. Las películas delgadas de $Sn_3Sb_2S_6$ muestran una transición óptica indirecta con brechas de energía cercanas a 1 eV, y coeficientes de absorción ~ 10^5 cm^{-1} en el rango del espectro visible. Las películas delgadas de $Sn_3Sb_2S_6$ muestran conductividades de 10^{-7} – 10^{-6} Wcm^{-1}, observándose un incremento en la conductividad conforme aumenta la temperatura. Las buenas propiedades optoelectrónicas obtenidas hacen que este material sea prometedor para aplicaciones fotovoltaicas.

Optoelectrónico, Semiconductor, Propiedades

Citation: GONZALEZ-GARZA, Jorge Oswaldo, GARCÍA-GUILLEN, Grisel, RÍOS-RAMÍREZ, Bernardino and DE RAMÓN-CONDÉ, Andres. $Sn_3Sb_2S_6$ thin films for photovoltaic applications. Journal of Innovative Engineering. 2023. 7-20: 16-21

*Correspondence to Author (e-mail: jorge.gonzalez@upgarcia.edu.mx)
† Researcher contributing as first Author.

1. Introduction

Thin film solar cell (TFSC) technology is based on copper indium gallium selenium (CIGS) and CdTe absorber materials, which have demonstrated the best efficiency conversion of sunlight into electricity in TFSC technology; efficiencies of 22.6% and 22.1%, have been reported for CIGS (Taoufik Chargui, 2023) and CdTe (E.I. Emon, 2023), respectively. The main drawback with these absorber materials is the scarcity of indium and gallium, and the toxicity of cadmium. In that fact, new absorber materials are being extensively studied, focusing on the availability of the constituent elements and low toxicity (Aiswarya Nadukkandy, 2023; Jiayou Xue, 2023). Ternary compounds base on tin antimony sulfide (TAS) sulfosalts family are good candidates as absorber materials for thin films solar cell technology.

The chemistry of this sulfosalt family is $A_xB_yX_z$, where A is the metallic atom such as tin (Sn^{2+}, Sn^{4+}), Iron (Fe^{2+}), etc. B corresponds to the metallic atoms like Antimony (Sb^{3+}), Arsenic (As^{3+}), and X is the anion such as Sulfur (S^{-2}), Selenium (Se^{2-}) (Sebin Devasia, 2020). Abdelkader *et al*. prepared $SnSb_4S_7$, $Sn_2Sb_6S_{11}$, $SnSb_2S_4$, $Sn_4Sb_6S_{13}$, $Sn_2Sb_2S_5$ and $Sn_3Sb_2S_6$ thin films by thermal evaporation of the corresponding $Sn_xSb_yS_z$ powders; the powders were obtained by crushing $Sn_xSb_yS_z$ ingots prepared by the Bridgman method. The optical properties of the TAS thin films were analyzed, the films showed high absorption coefficients in the visible region around 10^5 cm^{-1}, direct and indirect optical transitions, with band gaps in the range of 1.37 – 1.87 eV, depending on the chemical composition (D. Abdelkader, 2014). Bindu *et al*. prepared $Sn_6Sb_{10}S_{21}$ by heating chemically deposited multilayers of Sb_2S_3/SnS in vacuum; the thin films showed band gaps 1.26 – 1.45 eV, and high absorption coefficient 10^5 cm^{-1}, moreover, $Sn_6Sb_{10}S_{21}$ thin films were incorporated as absorber in a photovoltaic structure, the obtained cell parameter were: V_{oc} = 409 mV, J_{sc} = 1.46 mA/cm^2, and FF = 0.25 (Sebin Devasia, 2020).

To our knowledge there are no reports of the preparation $Sn_3Sb_2S_6$ by heating multilayers of SnS/Sb_2S_3 deposited by chemical bath deposition. The findings in this work are relevant and can contribute to the development of photovoltaic structures using this material as absorber.

2. Methods

2.1 Deposition of SnS thin films

SnS thin films were deposited on clean glass Corning substrates, that, previously to deposition, were washed with neutral detergent and rinsed with distilled water. For the deposition, 1 g of $SnCl_2$:$2H_2O$ was dissolved in 5 ml of acetone, and to this solution 12 ml of triethanolamine (3.7M) was added, followed by 65 ml of deionized water, 8 ml of thioacetamide (1M), and 10 ml of NH_3 (4M) (David Avellaneda, 2007). Cleaned glass substrates were placed vertically on a 100 ml beaker and the temperature was maintained at 40 °C for 20 h. Uniform SnS thin films of ~ 500 nm were obtained; thickness was measured using a Alpha-Step D-600 Stylus profiler.

2.2 Deposition of Sb_2S_3 thin films

On the glass/SnS structure Sb_2S_3 thin films were deposited. For this, 650 mg of $SbCl_3$ was dissolved in 2.5 ml of acetone in a 100 ml beaker, and then 25 ml of 1 molar $Na_2S_2O_3$ solution was added followed by 72.5 ml of precooled distilled water at 10 °C, the final solution was mixed for 30 s, and glass/SnS simples were placed vertically in the beaker for 4.5 h and maintained at 10 °C (J.O. Gonzalez, 2014), two consecutive deposits were done.

2.3 Heat treatment of glass/SnS/Sb_2S_3 multilayers

The glass/SnS/Sb_2S_3 multilayers were heated in a conventional non-vacuum furnace at 100°C, 150 °C, 200 °C, 250 °C, 300 °C and 325 °C in air for 1 h.

3. Results and Discussion

XRD diffractograms for the glass/SnS/Sb_2S_3 multilayers heated at 100 °C, 150 °C, 200 °C, 250 °C, 300 °C and 325 °C in air are shown in graphic 1. At 100 °C, 150 °C and 200 °C the samples show the formation of two phases, SnS and Sn_2S_3. Peaks at 2θ of 28.55° and 30.52° are indexed to the planes (1 1 2) and (0 1 3), respectively, and correspond to Ottemannite phase (Card. No. 9011236). A peak at 2θ = 31.54 ° corresponds to the plane (1 3 0) of the phase SnS (Card. No. 9008785).

ISSN 2523-6873

It is evident that at temperatures below 200 °C no diffusion of the Sn, S and Sb constituent elements occurs for the formation of the ternary $Sn_3Sb_2S_6$ thin films.

At a temperature of 250 °C we observe the formation of two additional phases, named Sb_2S_3 and $Sn_3Sb_2S_6$. Two peaks at 2θ of 24.94° and 27.62°, are indexed to the planes (1 1 4) and (4 0 9) and corresponds to the ternary phase of $Sn_3Sb_2S_6$ (Card. No. 1541641). The formation of the ternary phase $Sn_3Sb_2S_6$ is explained as follows: as the temperature increases the Sn, Sb and S species diffuses between SnS and Sb_2S_3 layers, the species diffuses from the higher concentration region to the lower concentration region and react according to the following proposed reactions: $3SnS + Sb_2S_3 \rightarrow Sn_3Sb_2S_6$ and $3Sn_2S_3 + 2Sb_2S_3 \rightarrow 2Sn_3Sb_2S_6 + 3S\uparrow$ (g). The intensity of the $Sn_3Sb_2S_6$´s peaks is low, indicating low crystallinity, additionally, it is evident unreacted SnS, Sn_2S_3 and Sb_2S_3 (denoted as "#" in the diffractogram, card. No. 9003459) phases, so a higher temperature is necessary for the complete reaction and formation of the ternary $Sn_3Sb_2S_6$ phase.

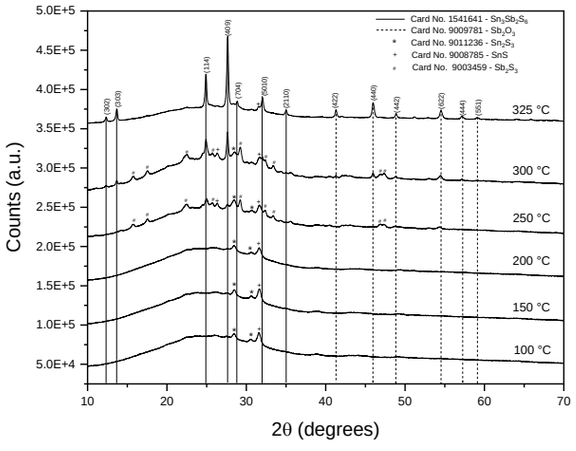

Graphic 1 XRD diffractograms of glass/SnS/Sb_2S_3 multilayers heated at 100 °C, 150 °C, 200 °C, 250 °C, 300 °C and 325 °C in air.

At a temperature of 300 °C, additional peaks of $Sn_3Sb_2S_6$ phase appear at 2θ = 12.36°, 13.68°, 31.99° and 34.98°, corresponding to the planes (3 0 2), (3 0 3), (5 0 10) and (2 1 10), respectively. Moreover, the intensity of the (1 1 4) and (4 0 9) increases, indicating an improvement of crystallization. In addition, it is evident the formation of Sb_2O_3 phase (Card. No. 9009781), this is due to the exposure of Sb_2S_3 with O_2 during heating.

Finally, at a temperature of 325 °C, peaks of $Sn_3Sb_2S_6$ phase increases in intensity, the intensity of these peaks is higher compared to the peaks of Sb_2O_3 phase, which indicates that $Sn_3Sb_2S_6$ is present as the major phase and Sb_2O_3 is the secondary one. No peaks of Sb_2S_3 and SnS phases are present at 325 °C, indicating that the reaction of the precursor layers is over and no more $Sn_3Sb_2S_6$ can be formed.

Crystal size of the thin films was calculated using the highest intensity peak by using the Scherrer´s formula given by:

$$D = \frac{0.9\lambda}{\beta cos\theta} \quad (1)$$

Where λ is the wavelength of the incident X-ray radiation (1.5406 Å), β is the full width at half maximum of the diffraction peak at 2θ, and D is the crystallite size (A. Harizi, 2016). The crystallite size were 20.8 nm, 35.5 nm, and 38.6 nm, for the multilayers heated at 250 °C, 300 °C, and 325 °C, respectively. The crystallite size increases as the temperature increases due to the sintering process, that is a thermally activated process in which diffusion of species from high concentration region to low concentration region takes place, and big grains grow at expense of small grains.

To determine the preferential orientation, the texture coefficient was calculated form the reflection planes by using the following formula (Mindong Zheng, 2016):

$$TC_{(hkl)} = \frac{I_{(hkl)} \Big/ I_{o(hkl)}}{\frac{1}{N}\sum_{N=1}^{N} I_{(hkl)} \Big/ I_{o(hkl)}} \quad (2)$$

Where $I_{(hkl)}$ and $I_{o(hkl)}$ are the measured and standard intensities, respectively, and N es the number of available diffraction peaks from the diffractogram. The preferred orientation for the samples heated at 250 °C, 300 °C and 325 °C were the planes (1 1 4), (5 0 10), and (5 0 10), respectively.

Graphic 2 shows the optical characteristics of the samples heated at 100 °C, 250 °C, 300 °C, and 325 °C. From the % transmittance and % reflectance measurements, the absorption coefficient was calculated using the following formula (J.O. Gonzalez, 2014):

ISSN 2523-6873

$$\alpha = \frac{1}{d} In \left[\frac{(1 - \%R)^2}{\%T} \right] \quad (3)$$

Where α is the absorption coefficient measured in cm^{-1}, d is the film thickness, in our experiments the measured thickness was ~ 1000 nm, %T is the percentage of transmittance and %R is the percentage of reflectance. In graphic 2 c) the absorption coefficients for the samples are shown, from the graphic is evident that all samples have high absorption coefficients ~ 10^5 cm^{-1} in the visible range, which means that small thickness is necessary to absorb most of the incident radiation.

From the spectra, the optical band gap of the samples was calculated using the formula, id.:

$$(\alpha h\nu)^{1/2} = A(h\nu - E_g) \quad (4)$$

Where E_g is the optical band gap, the exponent of ½ indicates an allowed indirect transition, α is the absorption coefficient at a frequency *v*, and A is a constant. From graphic 2 d), all samples showed band gaps near 1 eV.

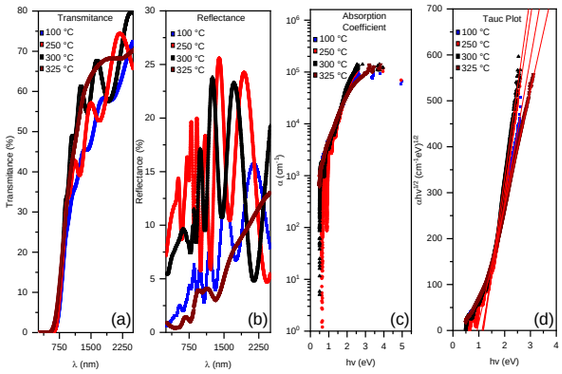

Graphic 2 Optical characteristics of samples heated at 100 °C, 250 °C, 300 °C, and 325 °C in air. a) % Transmittance, b) % Reflectance, c) Absorption coefficient, and d) Tauc plot.

Graphic 3 shows the electrical characteristics of the samples heated at 100 °C, 250 °C, 300 °C, and 325 °C. In the graphic, both, photocurrent and IV curves of the samples are shown. The IV curve of the samples follows the ohm´s law, in which, current and voltage varies linearly; this is, as voltage increases current increases.

We observe that conductivity of sample heated at 100 °C is higher than conductivities of samples heated at 250°C and 300 °C, this may be due to the formation of Sb_2S_3 phase these temperatures, which is a highly resistive material (Sarah Messina, 2009). For the samples heated at 250°C, 300°C and 325 °C the photo response and conductivity increases, this may be due to the formation of $Sn_3Sb_2S_6$ phase, additionally, as the temperature increases conductivity increases due to the increase of grain size and crystallinity of the ternary compound.

As grain size increases, defects in the material, such as voids, grain boundaries, etc, that act as traps, reduces, decreasing the probability of recombination and the mobility of carries is improved as well as conductivity. The photo response of the samples was carried out by applying a bias voltage of 20 V and measure the current at dark and under illumination, 20 s at dark, 20 s under illumination and again 20 s at dark. When samples are illuminated, electrons from the valence band are promoted to the conduction band by absorbing photons with energy equal or greater than the band gap, current is increased due to more carriers are available for conduction. All samples show good photoconductivity behavior.

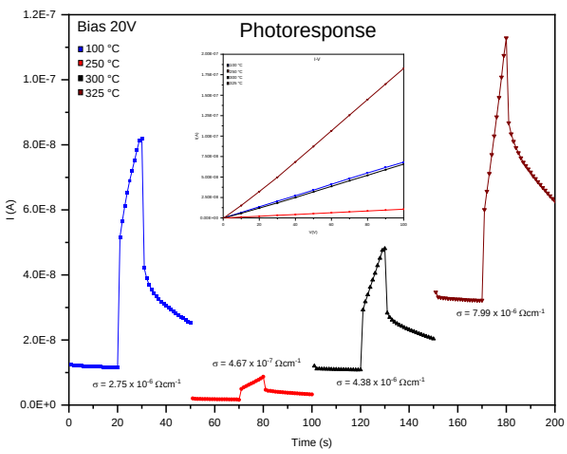

Graphic 3 Electrical characteristics of samples heated at 100 °C, 250 °C, 300 °C, and 325 °C in air.

4. Acknowledgements

The authors are thankful to Conacyt – Fondo Sectorial de Investigación para la Educación for financial support. Authors are thankful to Dr. David Avellaneda from FIME-UANL for Uv-Vis-IR measurements.

ISSN 2523-6873

5. Financing

This work has been funded by CONACYT [grant number A1-S-46032, 2017-2018].

6. Conclusions

$Sn_3Sb_2S_6$ thin films were prepared by heating multilayers of glass/SnS/Sb_2S_3 at different temperatures in air. XRD studies indicate that $Sn_3Sb_2S_6$ begins formation at 250°C, and a temperature of 325°C it is completely formed. Texture coefficient showed a preferential orientation along the (1 1 4) plane for sample heated at 250 °C and (5 0 10) plane for samples heated at 300°C and 325 °C. Optical properties of the films showed high absorption coefficients in the order of 10^5 cm^{-1}, and indirect allowed optical transitions with band gaps near 1 eV. The electrical properties of the samples were determined, samples showed conductivities in the order of 10^{-6} Ωcm^{-1}, and an improvement in the electrical conductivity for $Sn_3Sb_2S_6$ thin films was observed as temperature increases.

7. References

A. Gassoumi, M. K. (2011). Growth and post-annealing effect on the properties of the new sulfosalt SnSb2S4 thin films. *Physica E*, 71-74. doi:https://doi.org/10.1016/j.physe.2011.07.007

A. Harizi, M. B. (2016). Substrate temperature dependence of structural, morphological and optical properties of Sn4Sb6S13 thin films deposited by vacuum thermal evaporation. *Materials Research Bulletin*, 52-62. doi:https://doi.org/10.1016/j.materresbull.2016.02.043

A. Larbi, H. D. (2014). Effect of substrate temperature on structural and optical properties of the new high absorbent Sn3Sb2S6 thin films. *Vacuum*, 34-39. doi:https://doi.org/10.1016/j.vacuum.2014.08.009

Aiswarya Nadukkandy, S. S.-M. (2023). Cubic structured silver antimony sulfide-selenide solid solution thin films for sustainable photodetection and photovoltaic application. *Journal of Alloys and Compounds*, 169072. doi:https://doi.org/10.1016/j.jallcom.2023.169072

Auttasit Tubtimtae, P. P. (2021). Indium dopant-induced morphological and optical properties of tin-antimony sulfide thin films synthesized by spin coating method compared with ab initio calculation. *Materials letters*, 130140. doi:https://doi.org/10.1016/j.matlet.2021.130140

D. Abdelkader, M. B. (2014). Investigation on optical properties of SnxSbySz sulfosalts thin films. *Materials Science in Semiconductor Processing*, 14-19. doi:https://doi.org/10.1016/j.mssp.2014.01.027

David Avellaneda, G. D. (2007). Structural and chemical trasnformations in SnS thin films used in chemically deposited photovoltaic cells. *Thin solid films*, 5771 - 5776. doi:https://doi.org/10.1016/j.tsf.2006.12.078

E.I. Emon, A. I. (2023). A comprehesive photovoltaic study on tungsten disulfide (WS2) buffer layer based CdTe solar cell. *Heliyon*, e14438. doi:https://doi.org/10.1016/j.heliyon.2023.e14438

J.O. Gonzalez, S. S. (2014). Photovoltaic structures using AgSb(SxSe1-x)2 thin films as absorber. *Applied Physics A*, 2095 - 2105. doi:10.1016/j.solmat.2012.04.008

Jiayou Xue, X. Y. (2023). Improved Carrier Lifetimes of CdSe Thin Film via Te Doping for Photovoltaic Application. *ACS Applied Materials & Interfaces, 15*(14), 17858–17866. doi:https://doi.org/10.1021/acsami.3c00461

Mindong Zheng, J. N.-C. (2016). Effect of annealing temperatur on the crystalline structure, growth behaviour and properties of SnO2:Sb thin films prepared by radio frequency (RF)-magnetron sputtering. *Journal of Alloys and Compounds*, 371-378. doi:https://doi.org/10.1016/j.jallcom.2015.12.037

N. Ali, R. A. (2015). A novel approach for the synthesis of tin antimony sulphide thin films for photovoltaic application. *Solar Energy*, 25-33. doi:https://doi.org/10.1016/j.solener.2014.12.021

ISSN 2523-6873

Nisar Ali, S. H. (2013a). Effect of air annealing on the band gap and optical properties of SnSb2S4 thin films for solar cell application. *Materials Letters*, 148-151. doi:https://doi.org/10.1016/j.matlet.2013.02.097

Nisar Ali, S. H. (2013b). Structural and optoelectronic properties of antimony tin sulphide thin films deposited by thermal evaporation techniques. *Optik*, 4746-4749. doi:https://doi.org/10.1016/j.ijleo.2013.01.086

Sarah Messina, M. N. (2009). Solar cells with Sb2S3 absorber films. *Thin Solid Films*, 2503-2503. doi:https://doi.org/10.1016/j.tsf.2008.11.060

Sebin Devasia, S. S. (2020). Tin antimony sulfide (Sn6Sb10S21) thin films by heating chemically deposited Sb2S3/SnS layers: Studies on the structure and their optoelectronic properties. *Journal of Alloys and Compounds*, 154256. doi:https://doi.org/10.1016/j.jallcom.2020.154256

Taoufik Chargui, F. L.-H. (2023). Experimental and numerical study of the CIGS/CdS heterojunction solar cell. *Optical Materials*, 113849. doi:https://doi.org/10.1016/j.optmat.2023.113849

ISSN 2523-6873